Appl Phys B (2009) 97: 109–115
DOI 10.1007/s00340-009-3565-1

Applied Physics B
Lasers and Optics

Microbending loss and refractive index changes induced by transient thermal loading in double-coated optical fibers with thermal contact resistance

C.-L. Chu · H.-L. Lee · Y.-C. Yang

Received: 30 January 2009 / Published online: 9 May 2009

Abstract The transient microbending loss and refractive index changes in a double-coated optical fiber subjected to thermal loading with stress-dependent interlayer thermal contact resistance is investigated. The effects of interlayer thermal resistance on the transient microbending loss and refractive index changes of the optical fiber are analyzed and discussed. The results show that the stress-dependent interlayer thermal contact resistance will increase the lateral pressure induced by the transient thermal loading in the double-coated optical fiber and, thus, the microbending loss. Similarly, the interlayer thermal contact resistance will increase the transient thermal loading induced refractive index changes in the beginning of loading.

PACS 42.79.Wc · 44.10.+i · 68.65.Ac

1 Introduction

The conventional optical fiber for telecommunication is usually constructed of silica glass fiber coated by two or three layers of polymeric coatings [1, 2]. For an optical fiber containing two-layer coatings, usually the inner (or primary) coating is a soft polymer used as a strain buffer to minimize the microbending loss and the outer (or secondary) coating is a hard polymer used to increase the strength of the fiber. However, when silica fibers with polymeric coatings are stressed in a humid environment, strength degradation occurs after a long period of time due to slow crack growth. To solve this problem of moisture attack, inorganic coatings such as oxides, carbides, and carbon are being considered [3, 4]. On the other hand, metallic coatings such as aluminum, indium, copper, tin, ... etc. are also applied to the optical fibers [5–7]. Some of these fibers exhibit higher resistance to moisture attack and show higher strength than polymeric-coated fibers.

Thermal stresses occur in the optical fibers at a low temperature, which are due to the mismatches of thermal expansion properties of fiber and coating material [8, 9]. Thermal stresses are important in multilayer structures such as optical fibers, as they cause increased transmission loss in the optical fibers. Since thermal stresses affect the performance of the optical fibers, they have been extensively studied [10–16]. Nevertheless, to the authors' knowledge, there has been little work in the literature considering the effect of interlayer thermal contact resistance in such layered construction as optical fibers. In this article, we investigate the effect of interlayer thermal contact resistance on the transient temperature distributions, microbending loss, and refractive index changes in double-coated optical fibers, which are subjected to a sudden thermal loading. Furthermore, in this study, we do not assume a constant thermal contact resistance. Instead, a formula between the contact resistance and the normal stress is taken.

The stress-dependent interlayer thermal conductance will make the analysis more complicated, since a nonlinear thermal boundary condition relevant to this contact stress at interlayer is imposed on the linear heat conduction equation. Consequently, the temperature and displacement fields are related with each other. This implies that the heat conduction equation and equation of displacement compatibility

C.-L. Chu
Department of Mechanical Engineering, Nan Kai University of Technology, Nantou 542, Taiwan

H.-L. Lee · Y.-C. Yang (✉)
Department of Mechanical Engineering, Kun Shan University, Tainan 710, Taiwan
e-mail: ycyang@mail.ksu.edu.tw

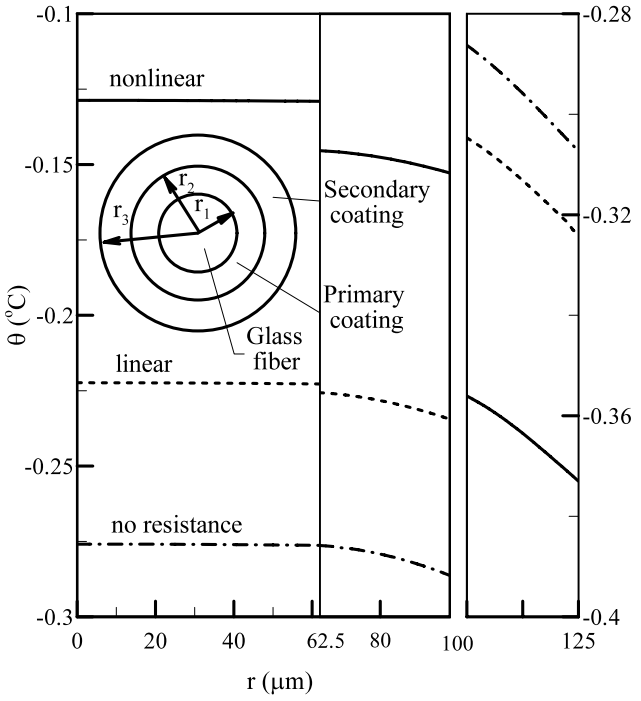

Fig. 1 Temperature drop θ distributions in the double-coated optical fiber at $t = 0.01$ second

are coupled and shall be dealt with simultaneously. After solving the coupled heat conduction equation and displacement compatibility equation, the transient temperature distributions, microbending loss, and refractive index changes in the double-coated optical fibers can be calculated.

2 Temperature distributions

Consider the transient heat conduction problem of a double-coated optical fiber as shown in Fig. 1. The optical fiber is constructed of a glass fiber coated by two-layer polymers, having radii of the fiber and the coating layers r_1, r_2, and r_3, respectively. Assume the double-coated optical fiber is initially at temperature $T_i(r, 0) = T_0$, and for time $t > 0$, the fiber at its boundary surface $r = r_3$ is subjected to a convective thermal loading of the surrounding temperature T_∞, $T_\infty < T_0$. Here the subscript $i = 1$ refers to the region of optical fiber, $i = 2$ refers to the region of primary coating, and $i = 3$ refers to the region of secondary coating, respectively. Define the temperature drop $\theta_i(r, t) = T_i(r, t) - T_0$; then the mathematical formulation of this transient heat conduction problem is given by [14]

$$\frac{\partial^2\theta_i(r,t)}{\partial r^2} + \frac{1}{r}\frac{\partial\theta_i(r,t)}{\partial r} = \frac{1}{\alpha_i}\frac{\partial\theta_i(r,t)}{\partial t}, \quad i = 1{-}3,\ 0 \le r \le r_3,\ t > 0, \tag{1}$$

$$\frac{\partial\theta_1(0,t)}{\partial r} = 0, \quad r = 0,\ t > 0, \tag{2}$$

$$k_1\frac{\partial\theta_1(r_1,t)}{\partial r} = k_2\frac{\partial\theta_2(r_1,t)}{\partial r}, \quad r = r_1,\ t > 0, \tag{3}$$

$$\theta_1(r_1,t) - \theta_2(r_1,t) = -R_1(p_1)k_1\frac{\partial\theta_1(r_1,t)}{\partial r}, \quad r = r_1,\ t > 0, \tag{4}$$

$$k_2\frac{\partial\theta_2(r_2,t)}{\partial r} = k_3\frac{\partial\theta_3(r_2,t)}{\partial r}, \quad r = r_2,\ t > 0, \tag{5}$$

$$\theta_2(r_2,t) - \theta_3(r_2,t) = -R_2(p_2)k_2\frac{\partial\theta_2(r_2,t)}{\partial r}, \quad r = r_2,\ t > 0, \tag{6}$$

$$-k_3\frac{\partial\theta_3(r_3,t)}{\partial r} = h\big[\theta_3(r_3,t) - \Delta T_\infty\big], \quad r = r_3,\ t > 0, \tag{7}$$

$$\theta_i(r,0) = 0, \quad t = 0, \tag{8}$$

where α, k, and h are the thermal diffusivity, thermal conductivity, and convection heat transfer coefficient, respectively, and $\Delta T_\infty = T_\infty - T_0$. R_1 is the interlayer thermal contact resistance at the interface of the glass fiber and the primary coating. R_2 is the interlayer thermal contact resistance at the interface of the primary coating and the secondary coating. In this article, a formula proposed by Tauchert et al. [17] is adopted for the interlayer thermal resistance R_1 and R_2, which is of the form

$$R_1(p_1) = S_1 + S_2\exp(S_3 p_1), \tag{9}$$

and

$$R_2(p_2) = S_4 + S_5\exp(S_6 p_2), \tag{10}$$

where $S_1{-}S_6$ are constants, p_1 is the lateral pressure at the interface of the glass fiber and the primary coating, and p_2 is the lateral pressure at the interface of the primary coating and the secondary coating. In addition, in the analysis, p_1 and p_2 are functions of time.

When we apply the Laplace transformation with respect to time to the problem of (1)–(8), the results will be

$$\frac{\partial^2\bar{\theta}_i}{\partial r^2} + \frac{1}{r}\frac{\partial\bar{\theta}_i}{\partial r} = \frac{1}{\alpha_i}s\bar{\theta}_i, \quad i = 1{-}3, \tag{11}$$

$$\frac{\partial\bar{\theta}_1(0,s)}{\partial r} = 0, \quad r = 0, \tag{12}$$

$$k_1\frac{\partial\bar{\theta}_1(r_1,s)}{\partial r} = k_2\frac{\partial\bar{\theta}_2(r_1,s)}{\partial r}, \quad r = r_1, \tag{13}$$

$$\bar{\theta}_1(r_1,s) - \bar{\theta}_2(r_1,s) = -R_1(p_1)k_1\frac{\partial\bar{\theta}_1(r_1,s)}{\partial r}, \quad r = r_1, \tag{14}$$

$$k_2\frac{\partial\bar{\theta}_2(r_2,s)}{\partial r} = k_3\frac{\partial\bar{\theta}_3(r_2,s)}{\partial r}, \quad r = r_2, \tag{15}$$

$$\bar{\theta}_2(r_2,s)-\bar{\theta}_3(r_2,s)=-R_2(p_2)k_2\frac{\partial\bar{\theta}_2(r_2,s)}{\partial r},\quad r=r_2, \tag{16}$$

$$-k_3\frac{\partial\bar{\theta}_3(r_3,s)}{\partial r}=h\big[\bar{\theta}_3(r_3,s)-\Delta T_\infty/s\big],\quad r=r_3, \tag{17}$$

where $\bar{\theta}_i(r,s)$ is the Laplace transformation of $\theta_i(r,t)$; s is the Laplace transformation parameter. Then applying the central finite difference technique in (11), we obtain the following discretized equations:

$$\frac{\bar{\theta}_{i,j-1}-2\bar{\theta}_{i,j}+\bar{\theta}_{i,j+1}}{\Delta r^2}+r_j^{-1}\frac{\bar{\theta}_{i,j+1}-\bar{\theta}_{i,j-1}}{2\Delta r}=\frac{1}{\alpha_i}s\bar{\theta}_{i,j}, \tag{18}$$

where Δr is the space increment, $j=1,2,\ldots,N$, and N is the total node number. Substituting boundary conditions of (12)–(17) into (18) and writing in matrix form, we obtain the following equation:

$$\big([A]-s[B]\big)[\bar{\theta}_{i,j}]=[Y], \tag{19}$$

where $[A]$ is a band matrix with real number, $[B]$ is a diagonal matrix of real number, $[\bar{\theta}_{i,j}]$ is a vector representing the unknown temperatures, and $[Y]$ is a complex vector representing the forcing terms. In general, we can obtain the solutions of all the nodal points in the transform domain by (19). However it is very involved to find the inverse Laplace transformation by the residue theorem. In this article, the inverse Laplace transformation is completed by a general method, known as the Fourier series technique [18]. On the other hand, the R values in matrix $[A]$ are calculated from the equations of displacement compatibility, which will be described later.

3 Lateral pressures

The double-coated optical fiber is simply subjected to thermal loading; while we assume that there is no stress in the fiber at the initial temperature, stress will be induced after the temperature drops. Since the problem is axisymmetric, the stress-strain relation in a zero strain condition is [19]

$$\begin{aligned}\varepsilon_\theta(r,t)&=\frac{u(r,t)}{r}\\&=\omega\cdot(1+\nu)\cdot\theta(r,t)+\frac{1-\nu^2}{E}\\&\quad\times\left[\sigma_\theta(r,t)-\frac{\nu}{1-\nu}\sigma_r(r,t)\right],\end{aligned} \tag{20}$$

where $u(r,t)$ is the radial displacement and r is the current radius. $\sigma_r(r,t)$, $\sigma_\theta(r,t)$, $\varepsilon_\theta(r,t)$, ω, ν, and E are the radial stress, tangential stress, tangential strain, effective thermal expansion coefficient, Poisson's ratio, and Young's modulus of the material, respectively.

The Lamé formula for the stress components in a circular thick-walled tube subject to internal pressure $p_i(t)$ and external pressure $p_e(t)$ are [19]

$$\sigma_r(r,t)=\frac{a^2p_i(t)-b^2p_e(t)}{b^2-a^2}+\frac{a^2b^2[p_e(t)-p_i(t)]}{(b^2-a^2)r^2}, \tag{21}$$

$$\sigma_\theta(r,t)=\frac{a^2p_i(t)-b^2p_e(t)}{b^2-a^2}-\frac{a^2b^2[p_e(t)-p_i(t)]}{(b^2-a^2)r^2}, \tag{22}$$

where a and b are the inner and outer radii of the tube. Substituting (21) and (22) into (20), we have

$$\begin{aligned}u(r,t)&=\omega\cdot(1+\nu)\cdot\theta(r,t)\cdot r+\frac{1+\nu}{E(1-\xi^2)}\\&\quad\times\big\{(1-2\nu)\big[\xi^2p_i(t)-p_e(t)\big]r\\&\quad-a^2\big[p_e(t)-p_i(t)\big]/r\big\},\end{aligned} \tag{23}$$

where $\xi=a/b$ is the ratio of the radii.

Using (23), we can obtain the radial displacement $u_{11}(r_1,t)$ of the glass fiber and the radial displacement $u_{21}(r_1,t)$ of the inner boundary of the primary coating, at $r=r_1$, as follows:

$$\begin{aligned}u_{11}(r_1,t)&=\omega_1\cdot(1+\nu_1)\cdot\theta_1(r_1,t)\cdot r_1\\&\quad-\frac{(1+\nu_1)(1-2\nu_1)r_1}{E_1}p_1(t),\end{aligned} \tag{24}$$

$$\begin{aligned}u_{21}(r_1,t)&=\omega_2\cdot(1+\nu_2)\cdot\theta_2(r_1,t)\cdot r_1+\frac{(1+\nu_2)r_1}{E_2(1-\xi_1^2)}\\&\quad\times\big\{(1-2\nu_2)\big[\xi_1^2p_1(t)-p_2(t)\big]\\&\quad-\big[p_2(t)-p_1(t)\big]\big\},\end{aligned} \tag{25}$$

where ω_1, E_1, and ν_1 are the effective coefficient of thermal expansion, Young's modulus, and Poisson's ratio of the glass fiber, respectively; ω_2, E_2, and ν_2 are the effective coefficient of thermal expansion, Young's modulus, and Poisson's ratio of the primary coating, respectively; $p_1(t)$ and $p_2(t)$ are lateral pressures at the interfaces of the glass fiber-primary coating and of the primary coating-secondary coating, respectively; $\xi_1=r_1/r_2$.

Similarly, the radial displacement $u_{22}(r_2,t)$ of the outer boundary of primary coating and the radial displacement $u_{32}(r_2,t)$ of the inner boundary of secondary coating, at $r=r_2$, are

$$\begin{aligned}u_{22}(r_2,t)&=\omega_2\cdot(1+\nu_2)\cdot\theta_2(r_2,t)\cdot r_2+\frac{(1+\nu_2)r_2}{E_2(1-\xi_1^2)}\\&\quad\times\big\{(1-2\nu_2)\big[\xi_1^2p_1(t)-p_2(t)\big]\\&\quad-\xi_1^2\big[p_2(t)-p_1(t)\big]\big\},\end{aligned} \tag{26}$$

$$u_{32}(r_2,t)=\omega_3\cdot(1+\nu_3)\cdot\theta_3(r_2,t)\cdot r_2+\frac{(1+\nu_3)r_2}{E_3(1-\xi_2^2)}\times\left[(1-2\nu_3)\xi_2^2+1\right]p_2(t),\tag{27}$$

where ω_3, E_3 and ν_3 are the effective coefficient of thermal expansion, Young's modulus, and Poisson's ratio of the secondary coating, respectively; $\xi_2=r_2/r_3$.

Using the compatibility conditions of displacement at interfaces, $u_{11}(r_1,t)=u_{21}(r_1,t)$ and $u_{22}(r_2,t)=u_{32}(r_2,t)$, we can obtain the formulas for $p_1(t)$ and $p_2(t)$. The lateral pressures $p_1(t)$ and $p_2(t)$ are proportional to the temperature drop θ_i at the interfaces and depend on the thickness and material properties of the coating layers. In this article, the compatibility conditions are solved simultaneously with (19) to determine $\theta_i(r,t)$, $p_1(t)$, and $p_2(t)$.

4 Normal stresses

The radial stress $\sigma_r(r,t)$ and tangential stress $\sigma_\theta(r,t)$ in the glass fiber can be obtained by setting $a=0$, $p_i(t)=0$, and $p_e(t)=p_1(t)$ in (21) and (22), they are

$$\sigma_r(r,t)=\sigma_\theta(r,t)=-p_1(t),\quad 0\le r\le r_1,\ t>0.\tag{28}$$

The axial strain is zero for the case of plain strain; and then the axial stress from the stress-strain relation is given by

$$\sigma_z(r,t)=E\omega\theta(r,t)+\nu\left[\sigma_r(r,t)+\sigma_\theta(r,t)\right].\tag{29}$$

Hence, the axial stress in the glass fiber is

$$\sigma_z(r,t)=E_1\omega_1\theta_1(r,t)-2\nu_1p_1(t),\quad 0\le r\le r_1,\ t>0.\tag{30}$$

5 Microbending loss

The compressive lateral pressure $p_1(t)$ in the glass fiber would produce excess microbending loss $\Gamma(t)$. Although this pressure is inevitable, it should be minimized. There exists a linear relationship between $p_1(t)$ and $\Gamma(t)$; that is

$$\Gamma(t)=Kp_1(t),\tag{31}$$

where K is a constant, and its value is approximately 0.02 (dB/km)/kpsi or 0.0029 (dB/km)/Mpa [20].

6 Refractive index changes

The refractive index would be changed when glass fiber is subjected to stress. The changes are given by [21]

$$\Delta n_r(r,t)=n_r-n=-B_2\sigma_r(r,t)-B_1\left[\sigma_\theta(r,t)+\sigma_z(r,t)\right],\quad 0\le r\le r_1,\ t>0,\tag{32}$$

$$\Delta n_\theta(r,t)=n_\theta-n=-B_2\sigma_\theta(r,t)-B_1\left[\sigma_r(r,t)+\sigma_z(r,t)\right],\quad 0\le r\le r_1,\ t>0,\tag{33}$$

$$\Delta n_z(r,t)=n_z-n=-B_2\sigma_z(r,t)-B_1\left[\sigma_r(r,t)+\sigma_\theta(r,t)\right],\quad 0\le r\le r_1,\ t>0,\tag{34}$$

where n is the refractive index of the unstressed glass fiber, n_r, n_θ, and n_z are the refractive indices of light rays. B_1 and B_2 are the stress-optical coefficients for the ordinary and extraordinary rays, respectively; the values are $B_1=4.2\times10^{-6}$/Mpa and $B_2=6.5\times10^{-7}$/Mpa, respectively [22].

7 Results and discussions

The main purpose of this paper is to investigate the effect of the interlayer thermal resistance on the transient temperature distributions, microbending loss, and refractive index changes in a double-coated optical fiber, which is subjected to sudden thermal loading. Therefore, an example with $T_0=21°$C and $T_\infty=20°$C will be illustrated. In other words, the double-coated optical fiber, which has an initial temperature of 21°C, is assumed to be suddenly subjected to a thermal loading of constant surrounding temperature 20°C. The material properties and radii of the double-coated optical fiber are listed as follows [11, 17]:

$r_1=62.5\ \mu$m, $r_2=100\ \mu$m, $r_3=125\ \mu$m,

$\nu_1=0.17$, $\nu_2=0.49$, $\nu_3=0.44$,

$E_1=72.5$ GPa, $E_2=200$ MPa, $E_3=1.2$ GPa,

$\omega_1=0.56\times10^{-6}/°$C, $\omega_2=20\times10^{-6}/°$C,

$\omega_3=90\times10^{-6}/°$C,

$k_1=1.1$ w/m $\cdot\,°$C, $k_2=0.209$ w/m $\cdot\,°$C,

$k_3=0.149$ w/m $\cdot\,°$C,

$\alpha_1=5.9\times10^{-5}$ m^2/s, $\alpha_2=0.21\times10^{-5}$ m^2/s,

$\alpha_3=0.11\times10^{-5}$ m^2/s,

$S_1=0.00021$ m$^2\cdot$K/W, $S_2=0.0012$ m$^2\cdot$K/W,

$S_3=0.521$ MPa^{-1}, $S_4=0.00086$ m$^2\cdot$K/W,

$S_5=0.0021$ m$^2\cdot$K/W, $S_6=0.605$ MPa^{-1}.

Figures 1, 2, 3 depict the temperature drop distributions, $\theta_i(r,t)$, at $t=0.01, 0.02$, and 0.04 s, respectively, in the double-coated optical fiber along the radial direction. Two different dashed lines refer to the cases with constant thermal contact resistance (abbreviated hereafter as linear case) and without thermal contact resistance (abbreviated hereafter as no resistance), respectively; while the solid lines refer to the case with stress-dependent thermal contact resistance (abbreviated hereafter as nonlinear case). For the

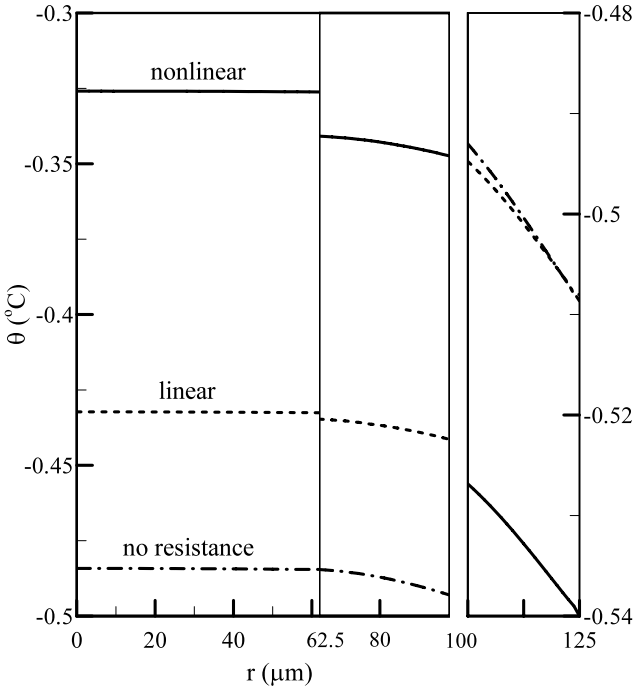

Fig. 2 Temperature drop θ distributions in the double-coated optical fiber at $t = 0.02$ second

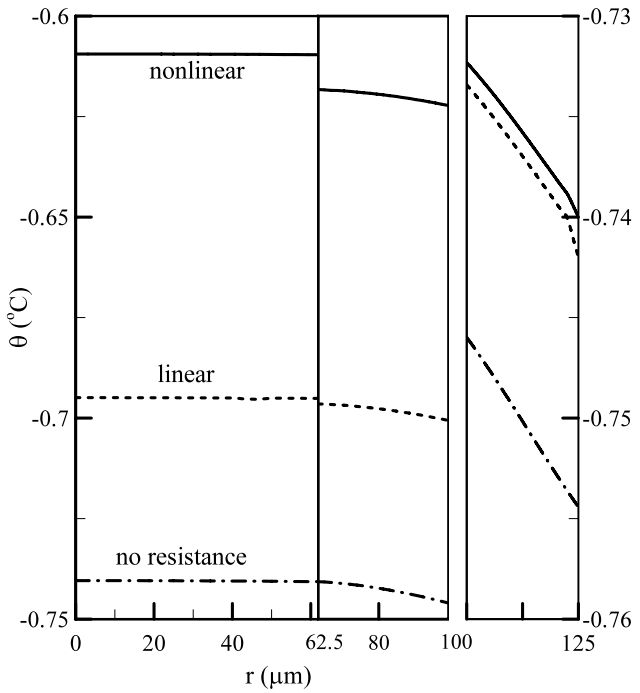

Fig. 3 Temperature drop θ distributions in the double-coated optical fiber at $t = 0.04$ second

linear case the values of the thermal resistance R_1 and R_2 are equal to 0.00021 and 0.00086, respectively. For the no resistance case the temperature drop is continuous at the interface, whereas a discontinuity in the value of the temperature drop is found for both the linear and nonlinear cases. It can be seen from (4) and (6) that, in general, the magnitude of this discontinuity in temperature increases with increasing value of interlayer thermal resistance and the amount of heat flux across the interlayer. Figures 1, 2, 3 also show that there exists a discrepancy in the temperature drop distributions, $\theta_i(r, t)$, among the above three cases, which coincides with our expectation. On the other hand, the temperature drop increases with the increase of radius. Moreover, the interlayer thermal contact resistance will decrease the temperature drop in the glass fiber and primary coating, since the existence of the thermal contact resistance will decrease the heat flux from the glass fiber to the primary coating and from the primary coating to the secondary coating.

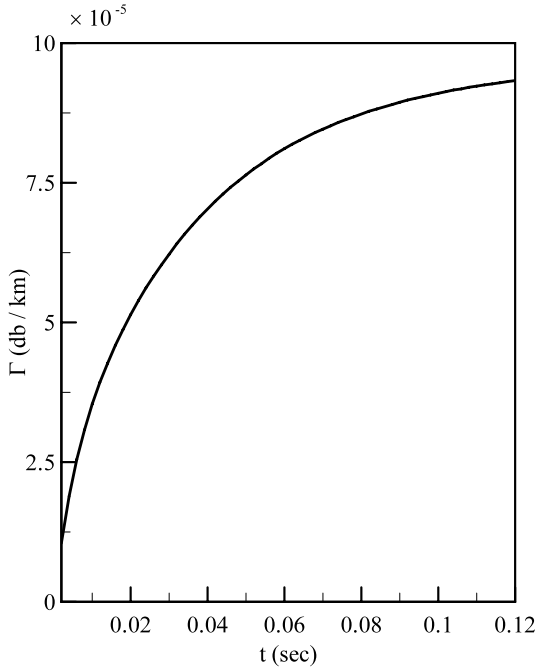

Fig. 4 Variation of microbending loss Γ with time t for the nonlinear case

Figure 4 illustrates the variation of microbending loss with time for the case with stress-dependent thermal contact resistance. It shows that the microbending loss of the carbon-coated optical fiber increases with the increasing time, which means that the compressive lateral pressure at the interface also increases with the increase of time. On the other hand, the effect of interlayer thermal contact resistance on the microbending loss is depicted in Fig. 5, in which DIF1(t) and DIF2(t) are defined as

$$\mathrm{DIF1}(t) = \frac{\Gamma_{\mathrm{lin}}(t) - \Gamma_{\mathrm{non}}(t)}{\Gamma_{\mathrm{non}}(t)} \times 100\%,$$

$$\mathrm{DIF2}(t) = \frac{\Gamma_{\mathrm{nor}}(t) - \Gamma_{\mathrm{non}}(t)}{\Gamma_{\mathrm{non}}(t)} \times 100\%,$$

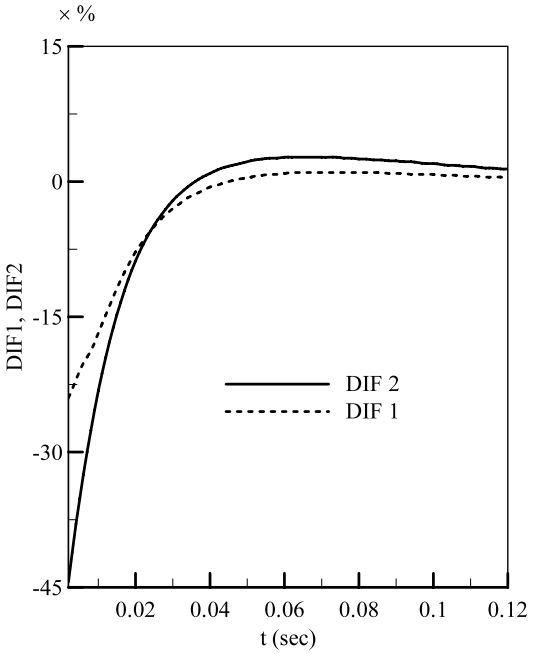

Fig. 5 Variation of DIF1 and DIF2 with time t

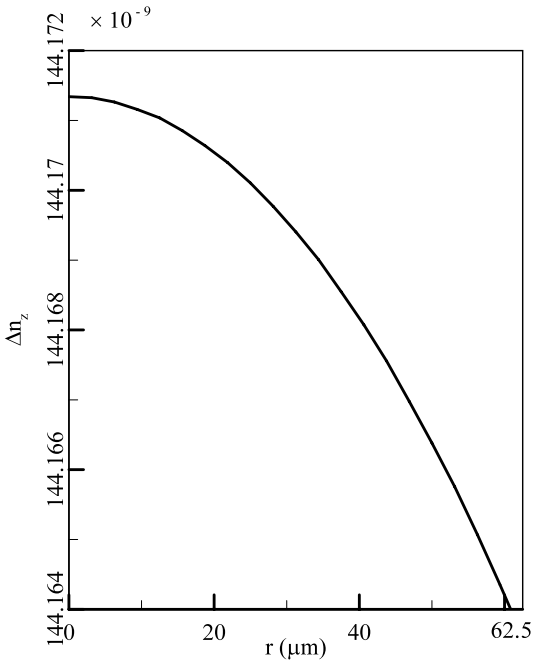

Fig. 7 Refractive index changes Δn_z distributions in the double-coated optical fiber at $t = 0.02$ second

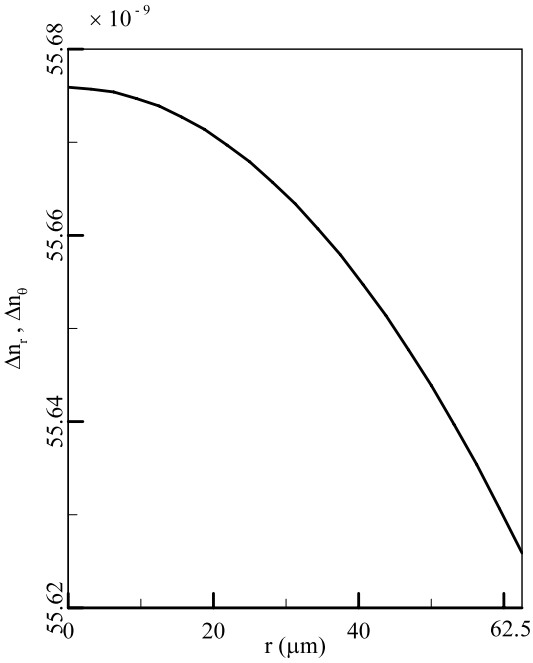

Fig. 6 Refractive index changes Δn_r and Δn_θ distributions in the double-coated optical fiber at $t = 0.02$ second

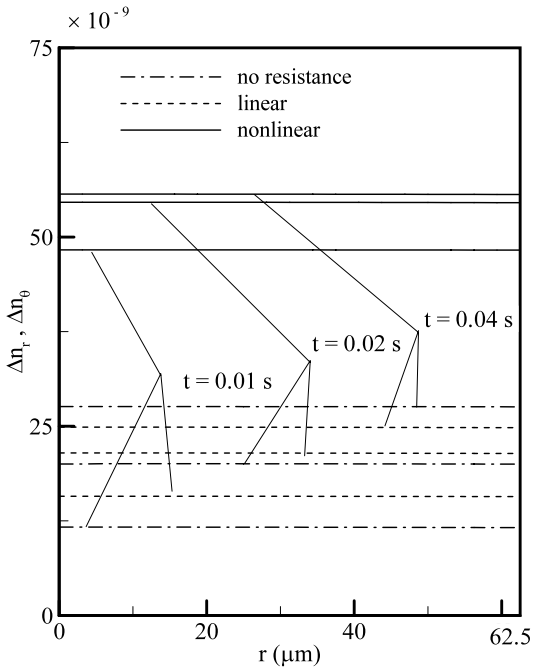

Fig. 8 Refractive index changes Δn_r and Δn_θ distributions in the double-coated optical fiber at various times

respectively. Here $\Gamma_{\text{non}}(t)$, $\Gamma_{\text{lin}}(t)$, and $\Gamma_{\text{nor}}(t)$ denote the microbending loss of the nonlinear, linear, and no resistance cases, respectively. Figure 5 shows that the microbending loss of the linear and no resistance cases is lower than that of the nonlinear case in the beginning of the thermal loading. In other words, the existence of stress-dependent thermal contact resistance will increase the microbending loss of the optical fiber in the transient state. Nevertheless, as time progresses, the difference will decrease gradually.

Figures 6, 7, 8, 9 illustrate the transient refractive index changes Δn_r, Δn_θ, and Δn_z of the glass fiber at various times along the radial direction, respectively. It can be

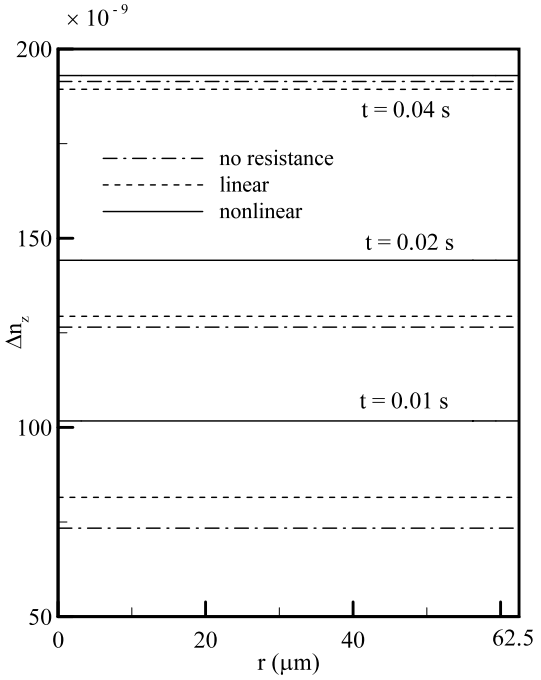

Fig. 9 Refractive index changes Δn_z distributions in the carbon-coated optical fiber at various times

found that the refractive index changes decrease with the increasing radius but increase with the increasing time. Moreover, the refractive index changes of the nonlinear case are higher than those of both the linear and no resistance cases. In other words, the existence of a stress-dependent thermal contact resistance will increase the transient refractive index changes Δn_r, Δn_θ, and Δn_z.

8 Conclusion

The transient effects of interlayer thermal contact resistance on the microbending loss and refractive index changes of double-coated optical fibers, subject to sudden thermal loading, are investigated. The results show that the stress-dependent interlayer thermal contact resistance affects the microbending loss and refractive index changes in the same direction. In other words, it will increase the transient thermal loading induced lateral pressure in the double-coated optical fibers and, thus, the microbending loss. Similarly, the interlayer thermal resistance will also increase the transient thermal loading induced refractive index changes.

Acknowledgements This work was supported by the National Science Council, Taiwan, Republic of China, under the grant numbers NSC 97-2221-E-168-017 and NSC 97-2221-E-168-039.

References

1. N. Yoshizawa, Y. Katsuyama, Electron. Lett. **25**, 1429 (1989)
2. N. Yoshizawa, H. Tada, Y. Katsuyama, J. Lightwave Technol. **9**, 417 (1991)
3. A.H. Lettington, C. Smith, Diam. Relat. Mater. **1**, 805 (1992)
4. D.R. Biswas, Optim. Eng. **31**, 1400 (1992)
5. D.R. Biswas, S. Raychaudhuri, in *Technical Digest Optical Fiber Communication Conference* (1985), p. 124
6. T. Nozawa, D. Tanaka, A. Wada, R. Yamauchi, in *Technical Digest Optical Fiber Communication Conference* (1992), p. 217
7. V.A. Bogatyrjov, E.M. Dianov, S.D. Rumyantsev, A.A. Sysoliatin, in *Technical Digest Optical Fiber Communication Conference* (1993), p. 78
8. S.T. Shiue, J. Appl. Phys. **78**, 6384 (1995)
9. W.W. King, C.J. Aloisio, J. Electron. Packag. **119**, 133 (1997)
10. E. Suhir, J. Lightwave Technol. **6**, 1321 (1988)
11. W.J. Chang, H.L. Lee, Y.C. Yang, J. Appl. Phys. **88**, 616 (2000)
12. Y.C. Yang, Optim. Eng. **40**, 2107 (2001)
13. U.C. Chen, W.J. Chang, Optim. Eng. **41**, 1317 (2002)
14. Y.C. Yang, S.S. Chu, W.J. Chang, J. Appl. Phys. **95**, 5159 (2004)
15. H.L. Lee, Y.C. Yang, W.J. Chang, Appl. Phys. B Lasers Opt. **83**, 601 (2006)
16. Y.C. Yang, Opt. Commun. **278**, 81 (2007)
17. T.R. Tauchert, D.C. Leigh, M.A. Tracy, J. Press. Vessel Technol. **110**, 335 (1988)
18. H.L. Lee, H.M. Chou, Y.C. Yang, Energy Convers. Manag. **45**, 1749 (2004)
19. S.P. Timoshenko, J.N. Goodier, *Theory of Elasticity*, 3rd edn. (McGraw-Hill, New York, 1970), p. 56
20. E. Suhir, J. Lightwave Technol. **8**, 863 (1990)
21. G.W. Scherer, Appl. Opt. **19**, 2000 (1980)
22. W. Primak, D. Post, J. Appl. Phys. **30**, 779 (1959)